The Mechanism of the Luminescence of Solids

Ferd E. Williams and Henry Eyring

Citation: J. Chem. Phys. **15**, 289 (1947); doi: 10.1063/1.1746499
View online: http://dx.doi.org/10.1063/1.1746499
View Table of Contents: http://jcp.aip.org/resource/1/JCPSA6/v15/i5
Published by the AIP Publishing LLC.

single CC bond distances. The calculated values are 1.33A and 1.55A for the double and single bond distances, respectively. The experimental values are also 1.33A[7] and 1.55A,[7] respectively.

This very good agreement makes it of interest to attempt a more general expression for M which would then provide an expression suitable for all multiple bond distances. The form of Kavanau's relation [Eq. (2) of the text] indicates the choice $M=(n-1/n+1)^{\frac{1}{2}}$ which is satisfied for CC bonds where $n=2$. The relation $R=R_1[2/3+1/3(n-1/n+1)^{p/2}]$ is thus obtained.

Another relation which may be derived from this crude model is that between force constants of multiple CC bonds.

The potential energy of the double bond may be written as $(K_2/2)\Delta R_2^2$ for small displacements from the equilibrium position, where K_2 is the force constant of the double bond. From the figure, the energy can also be written as $(2K_1/2)\Delta R_1^2$ (since the tetrahedral angles are preserved) where K_1 is the single bond force constant. From (1) $\Delta R_1/\Delta R_2=\theta_1/\sin\theta_1$ whence $K_2=2K_1(\theta_1/\sin\theta_1)^2$. Similarly for triple bonds $K_3=3K_1(\theta_2/\sin\theta_2)^2$, where K_3 is the triple bond force constant. Putting in the values of θ_2 and θ_1 of 70.5° and 54.75° one obtains $K_3:K_2:K_1=5:2.7:1$ which is of the same order of accuracy as the ratio derived from Badger's rule,[7] *viz:* $K_3:K_2:K_1=5:2.5:1$.

That the circular bond notion with preserved tetrahedral angles is internally consistent is further demonstrated by the bond energy/bond distance relation which can be derived from it. (See Letter to the Editor, this Journal.)

Though this model was useful in obtaining relations which apparently represent the data, its success is totally unwarranted on the basis of present day valence theory. The author can suggest no reason for the apparent physical significance of this model.

The author takes pleasure in acknowledging the helpful discussions with members of the Yerkes Observatory of the University of Chicago.

THE JOURNAL OF CHEMICAL PHYSICS VOLUME 15, NUMBER 5 MAY, 1947

The Mechanism of the Luminescence of Solids*

FERD E. WILLIAMS**
RCA Laboratories, Princeton, New Jersey

AND

HENRY EYRING***
Princeton University, Princeton, New Jersey

(Received March 3, 1947)

In this paper, effort is directed toward explaining various diverse luminescent properties of solids in terms of a simple model of potential energy *versus* configuration coordinate. Three states of different multiplicities—a normal, metastable and an emitting state—are involved. The luminescent process consists of the excitation of an electron to the metastable level, the activated release of the electron to the emitting level, and a forbidden transition between the emitting and the ground state. With high excitation energy, the metastable state is bypassed. At high temperatures, the electron in the metastable state surmounts a larger potential barrier to undergo radiationless recombination with the activator atom.

Among those significant phenomena that have been measured experimentally and treated quantitatively by calculations based on this model are the temperature dependence of luminescent efficiency and the effect of type and wave-length of excitation on this temperature dependence; the three types of phosphorescence—spontaneous, metastable, and recombination phosphorescence; the phenomena of two-stage afterglow and the effect of type of excitation and temperature on the two stages; the

* Part of a dissertation submitted by Ferd E. Williams to Princeton University in partial fulfillment for the degree of Doctor of Philosophy. Portions of this article are based upon work performed for the Office of Scientific Research and Development under Contract NDCrc-150 and Contract OEMsr-440. Presented in part at the American Physical Society Meeting in New York in January, 1946.

** Now Assistant Professor of Chemistry, University of North Carolina, Chapel Hill, North Carolina.
*** Now Dean of the Graduate School, University of Utah, Salt Lake City, Utah.

relationship between buildup and afterglow kinetics; and the release of electrons from metastable states by thermal energy. The concept of the Absolute Rate theory are used to clear up the essential criteria for the different types of afterglow.

A detailed theoretical analysis of "glow curves" is presented and quantitatively applied to improved glow curves obtained at linear rates of heating 100 times slower than those previously reported. The slower rates of heating allow one metastable level to be operative at a time. Both monomolecular and bimolecular mechanisms are treated, and it is concluded that glow curves result from discrete metastable states that are emptied thermally by predominantly monomolecular kinetics. The explicit expressions for the specific rate constants involved in the release of electrons from metastable states are calculated.

I. INTRODUCTION

INORGANIC crystalline luminescent solids, commonly referred to as "phosphors," possess the property of absorbing energy of a certain frequency and re-emitting part of the absorbed energy as radiant energy of another frequency. If, on removing the excitation, emission ceases within the time required for an ordinary atomic transition, the phenomenon is called fluorescence. If the emission persists longer, the phenomenon is called phosphorescence. Most phosphors are prepared by crystallizing at 600 to 2000°C highly purified substances to which 0.001 to a few percent of a foreign substance, or "activator," has been added.

Phosphors belong to the class of solids known as electronic semi-conductors. Electrons in a crystal move in a potential which is periodic in three dimensions. Bloch[1] and Wilson[2] have studied such a system, and neglecting the exchange forces between the electrons, the energy levels consist of broad bands of allowed energies, separated by broad bands of forbidden energies. In their states of lowest energy the electrons which do not form a complete valence group should be tightly bound and exactly fill up one of the bands of allowed energies in order that a substance be an electronic semi-conductor. More precise energy diagrams[3] contain narrow continuous bands lying in the forbidden region between the Bloch-Wilson bands. In these states, which are computed by the Heitler-London approximation, the excited electron and the positive hole it leaves in the lowest band—together called an "exciton"—are closely coupled and move together, transporting no charge.

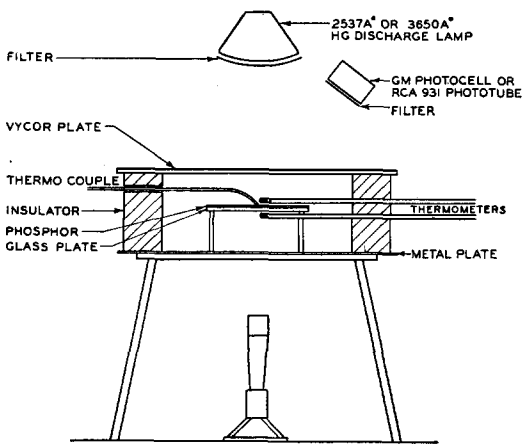

FIG. 1. Apparatus to measure the temperature dependence of efficiency of luminescence.

Impurities and crystal defects dominate the electrical properties of electronic semi-conductors.[4] An electron from a discrete impurity level just below the conduction band is more likely to be thermally excited to the conduction band than is an electron from the filled band. On introducing impurity ions into the lattice, the energies of the electrons on the ions are modified by the crystal field depending on the wave function for the state of each electron. Splitting[5] into sublevels according to symmetry considerations occurs. The interaction of levels of the impurity with lattice levels leads to the possibility of the formation of potential "wells" for trapping electrons.[3] Other proposed schemes for trapping electrons include trapping at crystal surfaces[6] and Landau trapping in which the electron essentially "digs its own hole."[7]

On exciting the impurity, there is no atomic rearrangement during the absorption process. After the absorption, the excited atom will have a different distribution of electronic charge, and

[1] F. Bloch, Zeits. f. Physik **52**, 555 (1928–29).
[2] A. H. Wilson, Proc. Roy. Soc. London **133**, 458 (1931).
[3] F. Seitz, J. Chem. Phys. **6**, 150 and 454 (1938).
[4] A. H. Wilson, Proc. Roy. Soc. London **134**, 277 (1932).
[5] H. Bethe, Ann. d. Physik **3**, 133 (1929).
[6] I. Tamm, Phys. Zeits. d. Sowjetunion **1**, 733 (1932).
[7] D. Blochinev, Comptes Rendus Acad. Sci. U.R.S.S. **2**, 79 (1934).

so, the atoms will shift to new equilibrium positions in the new force field, simultaneously radiating the excess energy as elastic waves. To describe completely this atomic rearrangement would require energy contours in a configuration space having three times as many coordinates as there are particles involved in the rearrangement. A useful simplification consists of defining a "center" as the excited atom plus the group of neighboring atoms involved in the rearrangement, and then specifying to a first approximation the coordinates of the center by an average configuration coordinate. Diagrams of potential energy *versus* configuration coordinate have been applied by Gurney and Mott,[8] Pringsheim,[9] and Seitz[3] to the phenomenon of luminescence of solids.

II. TEMPERATURE DEPENDENCE OF LUMINESCENT EFFICIENCY

The variation with temperature of the emission intensity under continuous excitation is a measure of luminescent efficiency and provides a key to the mechanism of luminescence. Such data obtained with ultraviolet excitation are simpler to measure experimentally and to interpret theoretically, and therefore, will be discussed first.

The measurements above and below 25°C were made on different apparatus. Figure 1 shows the furnace used for the measurements above 25°C. The emission intensity and temperature of the phosphor were simultaneously measured as the furnace was heated at a rate slow enough to keep the thermometers, above and below the sample, within 1C° of each other. The sulfide phosphors were excited by the 3650A G.E. E-H-4 100-watt lamp doubly-filtered with Corning 5840 and 5874. The borate, germanate, silicate, and tungstate phosphors were excited by the 2537A G.E. 8-watt germicidal lamp filtered with Corning 9863. Both lamps were operated from a voltage regulator to insure constant excitation intensity. The measurements were checked by taking points on the cooling curve as well as on the heating curve to test for any hysteresis effect. Runs were made with different Wratten filters on the photo-cell to determine whether

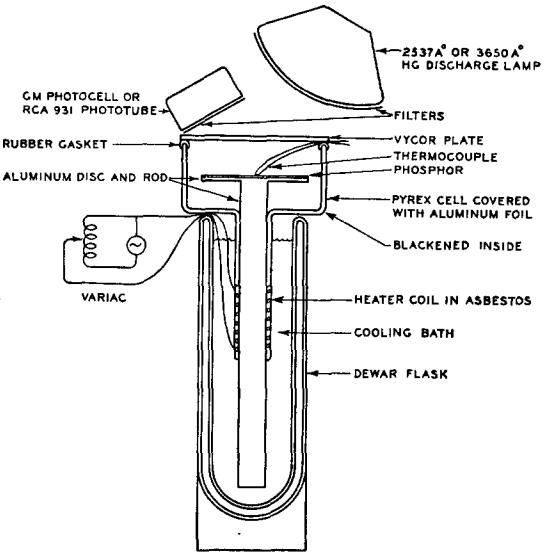

FIG. 2. Apparatus to measure "glow curves" and the temperature dependence of luminescent efficiency at low temperatures.

the emission spectrum has appreciable temperature dependence.

Figure 2 shows the apparatus used below 25°C. The lamps and filters were identical with the above. Before starting a run, the cell was desiccated by cooling by conduction with the liquid air in the Dewar flask. The phosphor on the aluminum disk was then inserted, the thermocouple dipped into the powder, and the apparatus allowed to attain thermal equilibrium. The Dewar flask was slowly lowered and with the current controlled by the Variac, a linear heating rate was approximated. The heating was continued above 25°C to allow a 50 C° overlap with the data taken on the high temperature apparatus.

The results may be summarized as follows: Above a rather critical temperature the luminescent efficiencies of the phosphors examined decrease rapidly and continuously with increasing temperature. The (Zn, Cd)S:Ag phosphors start to decrease in efficiency at 25°C and at 200°C the emission intensity is reduced to 10 percent. The (Zn, Cd)S:Cu phosphors increase in efficiency with increasing temperature until 225°C whereupon the efficiency starts to decrease and at 400°C has decreased to 10 percent of the efficiency at 25°C. The temperature-dependence curves of the borate, silicate, sulfoselenide, and

[8] R. W. Gurney and N. F. Mott, Trans. Faraday Soc. **35**, 69 (1939).
[9] P. Pringsheim, Rev. Mod. Phys. **14**, 132 (1942).

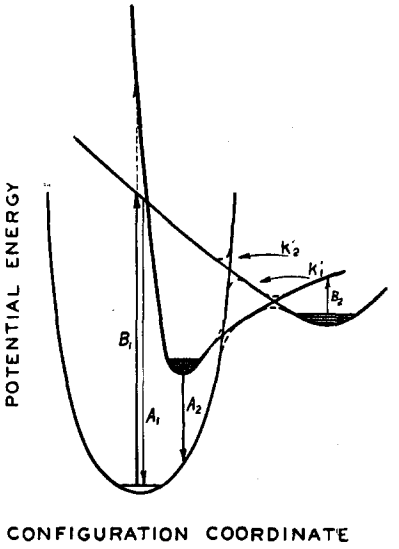

FIG. 3.

tungstate phosphors fell between these limits. The Zn_2SiO_4:Mn phosphor exhibits a slight hysteresis effect and two points of inflection as the efficiency decreases with increasing temperature. Below the rather critical temperature, the efficiencies of most of the phosphors decrease slowly with decreasing temperature.

The pronounced decrease of luminescent efficiency at high temperatures suggests an activated process with a large energy of activation by which excited electrons return to the ground state by a radiationless mechanism. The small decrease in efficiency at low temperatures can be explained by an activated step with a small energy of activation in the actual luminescent process. In other words, two competing processes are active: the radiationless recombination of the excited electron and center, and an activated step in the luminescent process.

To explain the temperature dependence of luminescent efficiency and many other diverse phenomena in the luminescence of solids, the model of potential energy *versus* configuration coordinate shown in Fig. 3 is proposed. The three states—the normal, the metastable, and the emitting states—represented by the contour lines, have different multiplicities: electrons in one state have a large probability of remaining in that state where the contours cross, and optical transitions between the states are to some extent forbidden. The metastable state is often referred to as an electron trap because activation of the electron in this state is necessary before emission can occur. With respect to the states of different multiplicities, the model is similar to the scheme proposed by G. N. Lewis[10] for the phosphorescence of organic molecules.

To calculate the temperature dependence of efficiency with continuous excitation to the metastable state, the following notation is introduced: n_1, n_2, and n_3 are the numbers of electrons in the normal, metastable, and emitting states, respectively; A_1 and A_2 are the transition probabilities for emission before and after trapping; B_1 and B_2 are the transition probabilities for excitation and for optical release from the electron trap; and k_1' and k_2' are the specific rate constants for surmounting the barriers between the metastable and the emitting state and between the metastable and the normal state. The rate constants for the reverse of the last two processes are negligible because of the

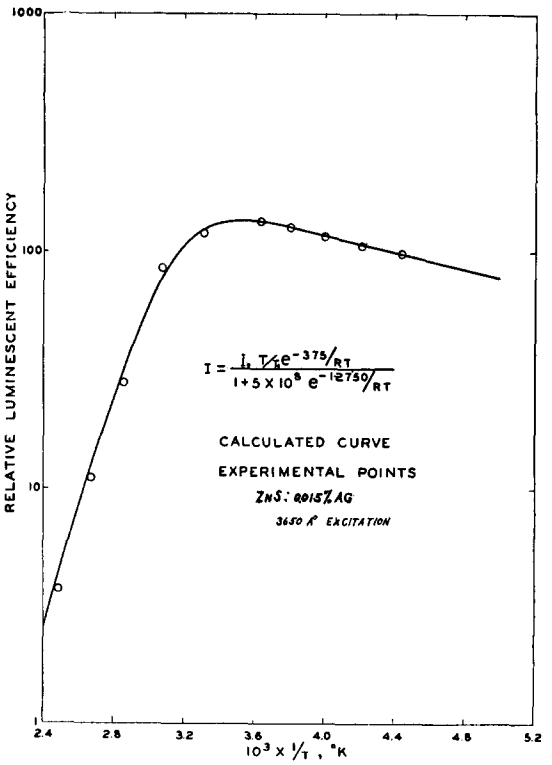

FIG. 4.

[10] G. N. Lewis *et al.*, J. Am. Chem. Soc. **63**, 3005 (1941); **64**, 1774 (1942); and **66**, 2100 (1944).

asymmetric character of the potential barriers. Applying the Stationary State Method, the following conditions result:

$$dn_3/dt = k_1'n_2 + B_2n_2 - A_2n_3 = 0,$$

$$dn_2/dt = -k_1'n_2 - k_2'n_2 + B_1n_1 - A_1n_2 - B_2n_2 = 0.$$

Combining these equations, the emission intensity can be written as follows after dividing by the non-temperature-dependent parameters:

$$I = \alpha(k_1' + B_2) \Big/ \left[1 + \frac{(k_1' + B_2)}{A_1} + \frac{k_2'}{A_1}\right].$$

In the absence of infra-red stimulation of suitable frequency to empty the metastable levels optically, the expression is simplified:

$$I = \frac{\alpha k_1'}{1 + k_1'/A_1 + k_2'/A_1}. \qquad (2\text{-}1)$$

According to the Absolute Rate theory,[11] the specific rate constants are of the following form:

$$k' = \kappa \frac{kT}{h} \exp(\Delta S^{\ddagger}/R) \exp(-\Delta H^{\ddagger}/RT). \qquad (2\text{-}2)$$

Substituting (2-2) in (2-1) and assuming that the transmission coefficient for the radiationless process is greater than the transmission coefficient for the activated step in the luminescent process, and that the entropy changes are small, the temperature dependence of the emission intensity takes the form:

$$I = \frac{I_0(T/T_0) \exp(-\Delta H_1^{\ddagger}/RT)}{1 + \beta \exp(-\Delta H_2^{\ddagger}/RT)}, \qquad (2\text{-}3)$$

where β is a constant dependent on A_1.

The experimental points and the curve calculated according to (2-3) are shown in Fig. 4 for the blue-emitting ZnS:Ag crystallized at 1240°C. The logarithm of emission intensity is plotted as a function of the reciprocal of the absolute temperature so that the slope of the straight-line portions of the curve are a measure of the heats of activation for the two competing processes. Similar results have been obtained with ZnS:Cu, ZnS:Mn, and $Cd_3(BO_3)_2$:Mn.

[11] S. Glasstone, K. J. Laidler, and H. Eyring, *The Theory of Rate Processes* (McGraw-Hill Book Company, Inc., New York, 1941).

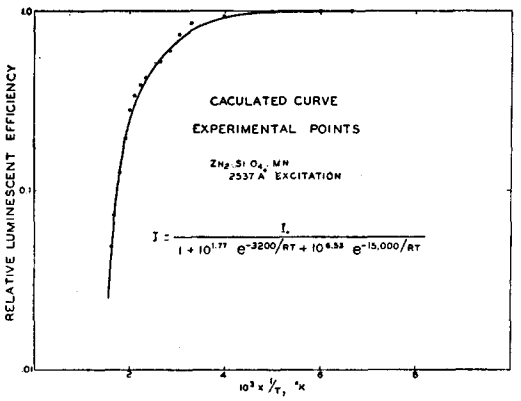

FIG. 5.

Generalizing (2-3) to include several possible mechanisms for the radiationless recombination of the excited electron and center, the following expression results:

$$I = \frac{I_0(T/T_0) \exp(-\Delta H_1^{\ddagger}/RT)}{1 + \sum_{j=2,3,\cdots} \beta_j \exp(-\Delta H_j^{\ddagger}/RT)}. \qquad (2\text{-}4)$$

With Zn_2SiO_4:Mn two possible mechanisms for the radiationless process of returning to the ground state are suspected because of the points of inflection in the region of the curve of luminescent efficiency *versus* temperature where the efficiency is decreasing rapidly with increasing temperature. The experimental points and the calculated curve based on (2-4) are shown in Fig. 5 for Zn_2SiO_4:Mn crystallized at 1200°C. The non-exponential factor for the radiationless process with the smaller heat of activation is unusually small.

In the case of the activated step in the luminescent process, there are also alternative mechanisms active. In fact, as is proven in Part V, there are electron traps of different depths active to different extents in the sulfide phosphors. During continuous excitation the shallower traps participate many times in the luminescent process compared to the deeper traps. Therefore, the depths of the shallow traps are statistically-weighted more than the depths of the deep traps in efficiency data, and the calculated heats of activation for release from the metastable state are only a few hundred calories.

From Fig. 3, it is clear that if the excitation

energy is sufficient to excite to the emitting state, then the electron trap will be bypassed and the luminescent efficiency would not be expected to decrease with decreasing temperature. This is consistent with the data of Schon[12] on the effect of wave-length of excitation on the temperature dependence of efficiency of (Zn, Cd)S:Zn and (Zn, Cd)S:Cu. For monochromatic excitation at 4047A or longer wave-lengths, the efficiency at 85°K is less than the efficiency at 298°K; whereas, for excitation at 3340A or shorter wave-lengths, the efficiency at 85°K is greater than the efficiency at 298°K.

The short wave ultraviolet or high energy corpuscular excitation resulting in a transition directly to the emitting state, in addition, leads to a different mechanism for the radiationless recombination of the excited electron and the center. The rate-determining step now involves surmounting the barrier connecting the emitting and the ground state. This mechanism probably requires a greater energy of activation than is involved in surmounting the barrier between the metastable and the ground state, otherwise it would have competed with the radiationless release from the trap with long wave excitation. This indicates that on excitation directly to the emitting state, the critical temperature, above which the luminescent efficiency decreases rapidly, will occur at a higher temperature than with excitation to the metastable state.

This interpretation was verified by measuring the temperature dependence of luminescent efficiency with excitation by 6 kv electrons. A demountable vacuum chamber was used. The phosphor, deposited on a platinum-plated Nichrome filament, was heated by passing current through the filament and was excited by a 60-cycle scanning electron beam. A 931 photomultiplier tube measured the emission intensity, and a Nichrome-Advance thermocouple measured the temperature of the phosphor. The inherent errors of measuring the temperature of an insulator in a vacuum prevented the results from being reliable to better than 10 percent, but it was concluded that the critical temperatures above which (Zn, Cd)S:Cu phosphors decrease in efficiency are higher with excitation by 6 kv electrons than by 3650A radiation. For example, the phosphor prepared according to the composition: 88 percent ZnS, 12 percent CdS, and 0.008 percent Cu, crystallized at 1220°C, and excited by 3650A ultraviolet has at 360°C only 10 percent the efficiency at 25°C. The same material excited by 6 kv electrons does not decrease to this efficiency until 510°C. This confirms our hypothesis regarding an alternative mechanism for the radiationless process on excitation directly to the emitting state.

[12] M. Schon, Naturwiss. **31**, 169 (1943).

III. PHOSPHORESCENCE

The model shown in Fig. 3 and used to explain the temperature dependence of luminescent efficiency is also consistent with various phosphorescent phenomena. The afterglow of various phosphors may be divided into spontaneous, metastable and recombination phosphorescence. The excited electron during spontaneous phosphorescence does not reach the conduction band but only reaches an excitation level and remains in the field of the center. The rate of emission of photons depends, therefore, only on the concentration of excited electrons and in the case of excited centers of only one kind reduces to monomolecular kinetics with the emission intensity expressed as follows:

$$I = -\alpha \frac{dn}{dt} = \alpha n_0 A e^{-At} \qquad (3\text{-}1)$$

where n and n_0 are, respectively, the numbers of excited electrons at times t and t_0. The transition probability A for spontaneous afterglow is only slightly influenced by temperature and depends on atomic selection rules perturbed by the lattice field.

The essential criterion for metastable afterglow is that the rate-determining step in the luminescent process is the thermal release of an electron from a metastable state or electron trap. If the electron passes through the conduction band on release from the trap, enhanced conductivity will occur. Because during the slow step each electron acts independently, the rate of emission will depend only on the concentration of excited electrons. Metastable phosphorescence requires an activation energy and is, therefore, strongly temperature dependent. In place of the

transition probability A in (3-1), a specific rate constant k' is substituted assuming the traps are of uniform depth:

$$I = -\alpha \frac{dn}{dt} = \alpha n_0 k' e^{-k't}. \qquad (3\text{-}2)$$

The rate constant is of the form (2-2).

If the excited electrons pass through the conduction band, each electron loses its relationship to its "own" center and if the rate-determining step is the migration of the electron through the conduction band, then the recombination of a center and an electron depends both on the concentration of ionized centers and on the concentration of conduction electrons. The decay of emission intensity proceeds by bimolecular kinetics if there are equal numbers of centers and electrons involved:

$$I = -\alpha \frac{dn}{dt} = \frac{\alpha k' n_0^2}{(1+n_0 k' t)^2}. \qquad (3\text{-}3)$$

As in metastable luminescence, k' is again expressed by (2-2).

Following the above introduction on phosphorescence, let us turn to some particular phosphors having interesting afterglow characteristics and interpret these characteristics in terms of our model. The fluorides will be discussed first. These phosphors are prepared from the metal oxides, including about one mole percent Mn, and excess HF acid in platinum apparatus and after drying are crystallized at 700 to 900°C. An alternative preparation is from the metal sulfate and KF.

The measurements of emission spectra and visual efficiencies were made with a spectroradiometer.[13] 6 kv and 1–5 μa/cm^2 d.c. electron excitation was used in these as well as in the phosphorescence measurements. The latter were made with a phosphoroscope[14] capable of automatic changes in sensitivity during the actual afterglow measurements. A 1P21 photo-multiplier picked up the phosphor emission and, after feeding into an oscilloscope, the trace was photographed. Corrections for the filament light and the irreducible ambient light were applied,

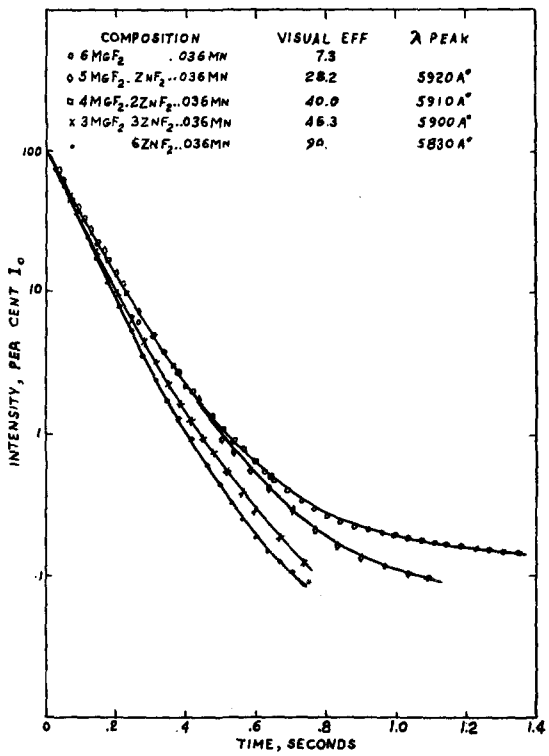

FIG. 6.

and finally the logarithm of intensity was plotted against time.

The (Zn, Mg)F_2:Mn phosphors have the longest, truly exponential afterglow of any of the efficient, known luminescent solids. The average lifetime of the excited state is $0.083 \pm .005$ second for ZnF_2:Mn and is $0.092 \pm .005$ second for MgF_2:Mn. In Fig. 6 are shown the afterglow curves for representative phosphors in this system. The concave-upward character of the phosphorescent curve is small but real. The emission spectra and relative visual efficiencies of several fluoride phosphors are shown in Fig. 7.

In the region of composition of 88 to 98 mole percent MgF_2 in the (Zn, Mg)F_2:Mn system, marked departure from exponential phosphorescence occurs as shown in Fig. 8. This type of phosphorescence can be accounted for by assuming that when excitation ceases, there are two sources of excited electrons which undergo luminescence by two different rate-determining steps.

In terms of the model shown in Fig. 3 the emitting state is the source of the initial expo-

[13] V. K. Zworykin, J. Opt. Soc. Am. 29, 84 (1939).
[14] R. E. Shrader, private communication.

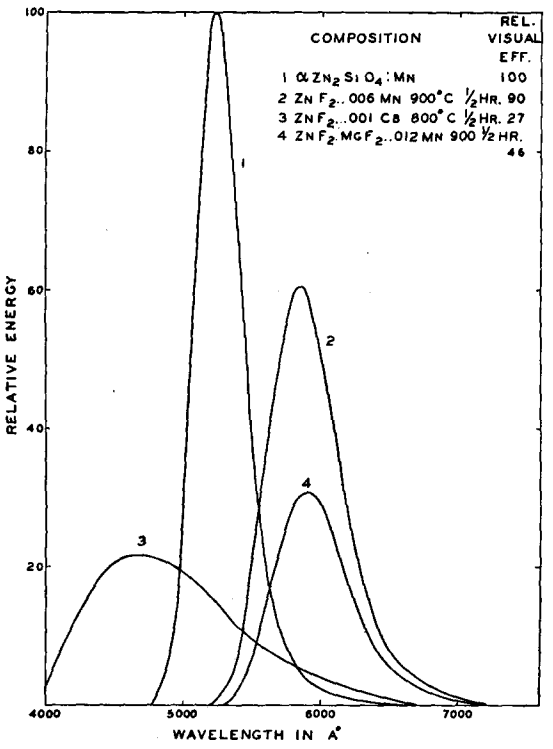

FIG. 7.

nential phosphorescence and the metastable state is the source of the slowly decaying phosphorescent tail. In addition to the notation used in Part II, n_{20} and n_{30} denote the numbers of electrons in the metastable and emitting states, respectively, when excitation ceases. The following conditions are obvious:

$$\frac{dn_3}{dt}=k_1'n_2-A_2n_3,$$

$$n_2=n_{20}\exp(-k_1't).$$

Combining the above and solving for n_3, the emission intensity is:

$$I=\alpha A_2n_3=\alpha A_2\left(\frac{n_{20}k_1'}{A_2-k_1'}-1\right)\times\exp(-k_1't)+\alpha n_{30}A_2e^{-A_2t}. \quad (3\text{-}4)$$

The application of (3-4) to the long persistent (Zn, Mg)F_2:Mn and to the ZnF_2:Mn is shown in Fig. 9. The long phosphorescence of the former and the slightly concave-upward character of the decay curve of the latter are precisely reproduced by the calculated expressions. The relative numbers of electrons in the metastable and emitting states when the excitation ceases can be determined from (3-4) or from the "light sums." Measurements of the temperature dependence of phosphorescence substantiate the somewhat arbitrary procedure of dividing the afterglow into two parts. The afterglow of ZnF_2:Mn is practically independent of temperature. The long phosphorescent tail of (Zn, Mg)F_2:Mn is latent at -78°C. After excitation by x-rays at this temperature, subsequent heating releases the electrons from the metastable state and light emission results. This is a "glow curve" of the type treated in Part V. The rate of the long-persistent afterglow increases with increasing temperature until at 250°C it equals that of the initial spontaneous afterglow. The heat of activation is about $4.5k$ cal.

$Cd_2P_2O_7$:Mn exhibits exponential phosphorescence with an average lifetime of the excited state of $0.040\pm.003$ second. The phosphate phosphors were prepared by precipitating $CdNH_4PO_4$

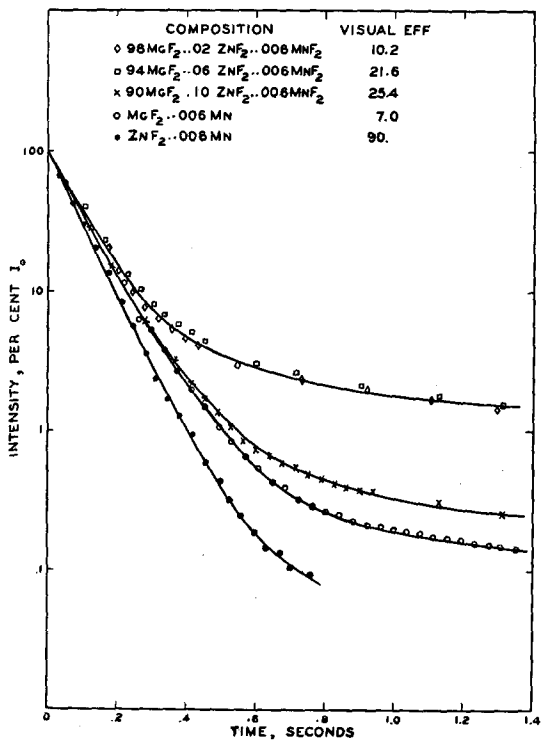

FIG. 8.

from $(NH_4)_2HPO_4$ solution with $Cd(NO_2)_2$, adding the activator as $Mn(NO_3)_2$, and crystallizing at 800 to 1000°C. The afterglow as shown in Fig. 10 depends to some extent on activator concentration and can be precisely reproduced by (3-4). The two curves can be fitted using the same two exponentials, with their individual contributions weighted differently. The initial afterglow may be associated with substitutional Mn and the slow phosphorescence with interstitial Mn.

Fonda[15] reports two-stage afterglow for Zn_2SiO_4:Mn with ultraviolet excitation and indicates that the second process may occur by bimolecular kinetics. In terms of Fig. 3 the data may be interpreted as an initial spontaneous process followed by a series of temperature-dependent monomolecular processes resulting from electron traps of different depths.

It is clear from Fig. 3 that the individual contributions to two-stage afterglow can also be resolved by using different types of excitation. The data of Leverenz[16] for Zn_2SiO_4:Mn indicate

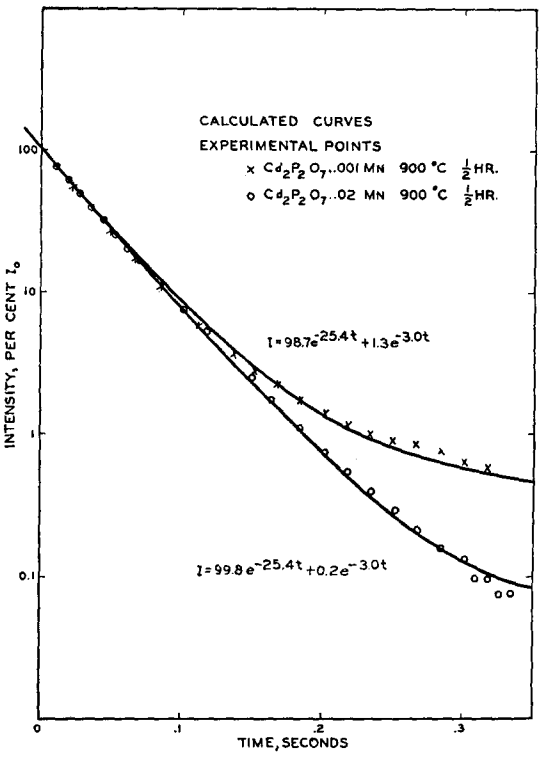

FIG. 10.

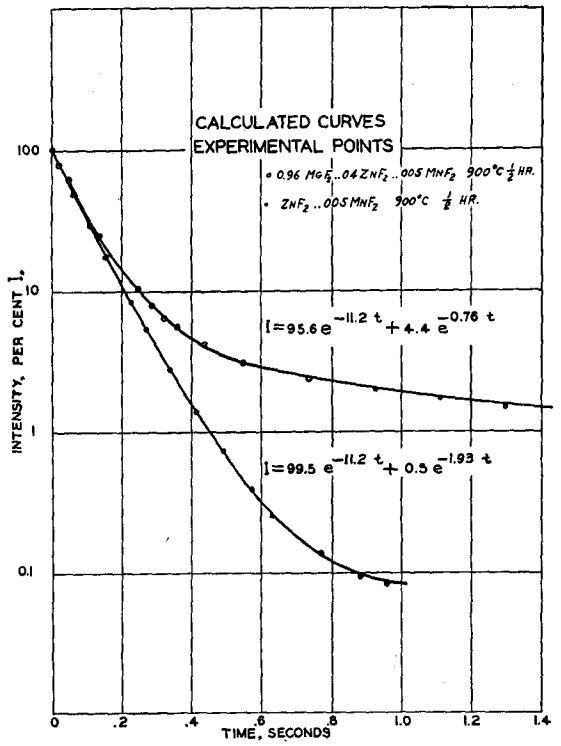

FIG. 9.

that excitation by 6 kv electrons results in the metastable state being bypassed so that even though excitation to the same emission intensity with electrons and ultraviolet can be attained, it is only with the radiation excitation that a temperature-dependent, phosphorescent tail persists. Leverenz explains this effect by localized heating by the cathode rays.

Antonov-Romanovsky[17] reports that KCl:Tl exhibits an initial, exponential afterglow only at low excitation intensities. This indicates a limited concentration of emitting states. The effect of infra-red radiation on the longer phosphorescence of this phosphor results in optical transitions from the metastable state.

An analysis of the data of Shrader[18] for SrS:Sm, Eu indicates that above 375°C a single metastable state with a thermal depth of 0.65 ev is active. This must correspond to the electron trap having an optical depth of 0.95 ev which can be emptied by 1.3μ radiation.

[15] G. R. Fonda, J. App. Phys. **10**, 408 (1939).
[16] H. W. Leverenz, RCA Rev. **7**, 199 (1946).
[17] V. V. Antonov-Romanovsky, J. Phys. U.S.S.R. **6**, 120 (1942); **7**, 153 (1943).
[18] R. E. Shrader, paper 15 at Optical Society of America Meeting at Cleveland (March, 1946).

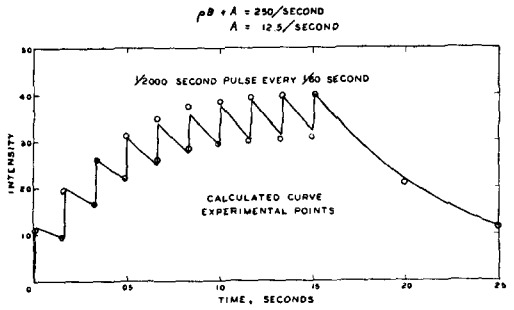

FIG. 11. $\rho B+A=250$/second, $A=12.5$/second.

IV. BUILD-UP OF LUMINESCENCE

The increase in emission intensity with time during initial excitation is referred to as build-up. Data on this property of phosphors have been reported by de Groot[19] for sulfides and by Fonda[15] for willemite.

The simplest build-up mechanism to analyze theoretically involves only a normal state and one excited state. In terms of Fig. 3 this means that the metastable levels participate only slightly and the kinetics are dominated by transitions between the ground state and the emitting state. Applying the notation used in Parts II and III, and introducing B and A as the transition probabilities for excitation and emission, ρ as the energy density of excitation, and n_0 as the total number of centers, the rate of change in the number of excited electrons is:

$$dn_3/dt=\rho B(n_0-n_3)-An_3.$$

Solving for the number of excited electrons:

$$n_3=\frac{\rho Bn_0}{(\rho B+A)}[1-e^{-(\rho B+A)(t-t_0)}]. \quad (4\text{-}1)$$

The emission intensity is therefore:

$$I=\alpha An_3=\frac{\alpha\rho BAn_0}{(\rho B+A)}[1-e^{-(\rho B+A)(t-t_0)}]. \quad (4\text{-}2)$$

On removing the excitation ρ at time t_1, n_3 decreases according to the following:

$$n_3=n_{31}e^{-A(t-t_1)}, \quad (4\text{-}3)$$

where n_{31} is the number of excited electrons at t_1. Substituting the explicit expression for n_{31} obtained from (4-1) in (4-3), the emission intensity during phosphorescence is:

$$I=\frac{\alpha\rho BAn_0}{(\rho B+A)}[1-e^{-(\rho B+A)(t_1-t_0)}]e^{-A(t-t_1)}. \quad (4\text{-}4)$$

The build-up and decay of emission intensity can be calculated for intermittent excitation by introducing the boundary values of n_3 into the solution of the proper differential equation at the beginning and end of each pulse. Introducing the notation:

$$f_m=e^{-(\rho B+A)(t_{m+1}-t_m)},$$

$$g_m=e^{-A(t_{m+1}-t_m)},$$

and noting that the excitation is first turned on at t_0, the emission intensity when the excitation is off is in general:

$$I=\frac{\alpha\rho BAn_0}{(\rho B+A)}(1-f_{m-1}\{1-g_{m-2}\times[1-f_{m-3}\cdots(1-g_1[1-f_0])]\})e^{-A(t-t_m)}, \quad (4\text{-}5)$$

where m denotes the number of times the excitation has either been turned on or off, and in (4-5) m is odd. The general expression for the build-up with pulsed excitation is as follows where m is even:

$$I=\frac{\alpha\rho BAn_0}{(\rho B+A)}(1-e^{-(\rho B+A)(t-t_m)}\{1-g_{m-1}\times[1-f_{m-2}\cdots(1-g_1[1-f_0])]\}). \quad (4\text{-}6)$$

Comparing (4-5) and (4-6), it is interesting to note that the rate constant for build-up may be

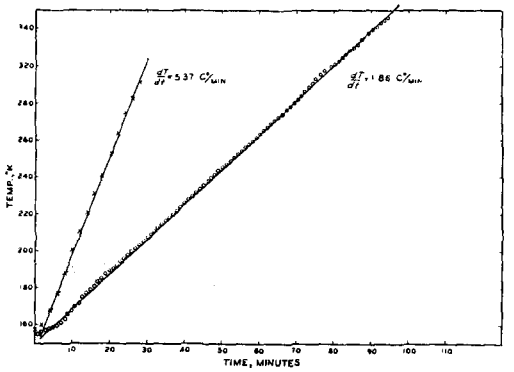

FIG. 12.

[19] W. de Groot, Physica 6, 275 (1939).

strongly dependent on the density of exciting radiation but the rate constant for phosphorescence is not. The latter must be less than or equal to the former. Insofar as the rate constant for build-up depends on excitation intensity, the emission will tend to become independent of the continuous excitation intensity. On the other hand, if $A \gg \rho B$ then the number of excited centers will be small compared to the number of available centers and the emission intensity will be proportional to the excitation intensity.

The data of Fonda[15] indicate that the latter conditions are approximately satisfied for the build-up and initial afterglow of willemite with 2537A excitation. The small contribution of the metastable process is probably responsible for the small differences in the rate constants for build-up and initial phosphorescence.

A better test of (4-5) and (4-6) is the build-up and phosphorescence of ZnF_2:Mn. The calculated curve and experimental points for pulsed build-up and afterglow are shown in Fig. 11. The measurements were made with the phosphoroscope[14] described in Part III. Ten 1/2000 second pulses of electrons were applied at 1/60 second intervals. The average excitation current was 175 μa/cm^2 during the individual pulses and the voltage was 6 kv. This high excitation intensity, coupled with the long lifetime of the excited state of ZnF_2:Mn, indicates that quite a large fraction of the available centers exist in the excited state. It is, therefore, not surprising that the rate constant for build-up $\rho B + A$ required to fit the data is twenty times the rate constant for phosphorescence A under these conditions of excitation. The slight deviation of the calculated curve from the experimental points is caused by a combination of experimental error and a small contribution from metastable luminescence. The analysis culminating in Eqs. (4-5) and (4-6) predicts at high excitation intensity the dependence of the rate constant for build-up on excitation intensity, the larger rate constant for build-up than for afterglow, and the lack of dependence of the rate constant for phosphorescence on intensity of excitation. The last two characteristics have been verified experimentally in the case of ZnF_2:Mn.

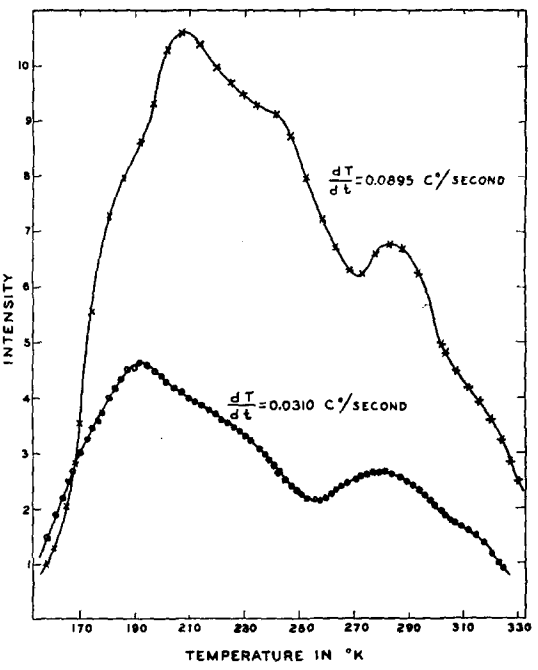

FIG. 13.

V. GLOW CURVES

For a phosphor exhibiting monomolecular, temperature-dependent phosphorescence, the depth of the metastable level is readily calculated from the temperature coefficient of the rate of decay of emission intensity. The afterglow of sulfide phosphors, however, does not vary as a simple function of temperature but tends to have a small irregular temperature dependence. This, coupled with the hyperbolic t^{-n} afterglow, indicates that a more complex type of phosphorescence is active. A possible explanation is that the metastable states or electron traps are not uniform in depth.

"Glow" data are useful in determining the mechanism of complex afterglow. A "glow curve" is obtained by exciting the phosphor, allowing the emission intensity to decay to a low value, and then measuring the emission intensity as the phosphor is heated, preferably at a linear rate. Urbach[20] first reported glow measurements on KCl:Tl, and Randall and Wilkins[21] reported and analyzed glow curves for sulfides assuming various distributions of electron traps. The rates

[20] F. Urbach, Akad. Wiss. Wien **139** IIa, 363 (1930).
[21] J. T. Randall and M. H. F. Wilkins, Proc. Roy. Soc. **A184**, 347, 366, 390 (1945).

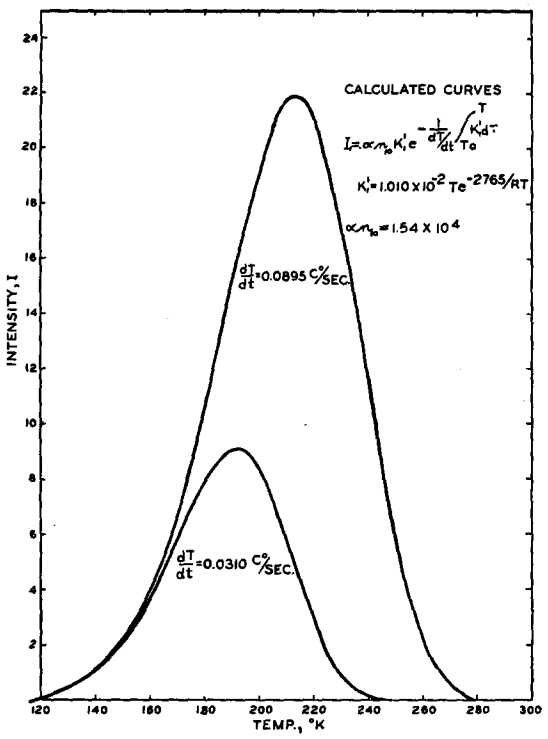

FIG. 14.

of heating used for ZnS:Cu and KCl:Tl varied from 2 to 10°C per second. Such fast heating rates do not allow metastable states of uniform depth to be exclusively operative at one time, but instead electrons from many traps of different depths contribute to the emission intensity.

The glow curves herein reported were obtained with linear heating rates about 100 slower than those previously reported. The apparatus shown in Fig. 2 was adapted to glow measurements. By adjusting the Dewar position and heating current, a constant rate of heating was maintained. Two heating cycles are shown in Fig. 12 and the corresponding glow curves are shown in Fig. 13 for ZnS activated with 0.003 percent Cu and crystallized at 1240°C. The phosphor was excited at 150°K with 3650A; the emission was detected with a 931 photo-multiplier; and the photocurrent was read on an ultra-sensitive d.c. ammeter. Readings of time, temperature, and intensity were taken simultaneously.

In treating the case of metastable states of uniform depth emptying by a monomolecular, rate-determining step, and producing luminescence without retrapping, the following notation is introduced: n_1 and n_{10} as the numbers of electrons in the metastable state at times t and t_0, and k_1' as the specific rate constant for surmounting the potential barrier between the metastable and emitting state. Solving the equation for the rate of decrease of trapped electrons:

$$n_1 = n_{10} \exp\left(-\int_{t_0}^{t} k_1' dt\right). \tag{5-1}$$

Introducing the rate of heating, the emission intensity is:

$$I_1 = -\alpha \frac{dn_1}{dt} = \alpha n_{10} k' \times \exp\left(-\frac{1}{dT/dt}\int_{t_0}^{t} k_1' dT\right). \tag{5-2}$$

Solving (5-1), expanding the logarithmic function, and introducing the rate of heating:

$$\int_{t_0}^{t} k_1' dT = -\ln\left[1-\left(\frac{n_{10}-n_1}{n_{10}}\right)\right] = \frac{dT}{dt}\left[\sum_{j=1}^{\infty}\frac{1}{j}\left(\frac{n_{10}-n_1}{n_{10}}\right)^j\right]. \tag{5-3}$$

Assuming that a negligible number of trapped electrons undergo radiationless recombination with the excited center or are retrapped, n_{10} and n_1 can be expressed in terms of the "light sums," so that (5-3) can be solved for k_1' as a function of observables:

$$k_1' = \frac{d}{dT}\left\{\frac{dT}{dt}\left[\sum_{j=1}^{\infty}\frac{1}{j}\left(\frac{\int_{T_0}^{T} I_1 dT}{\int_{T_0}^{\infty} I_1 dT}\right)^j\right]\right\}. \tag{5-4}$$

With (5-4) and an experimental glow curve resulting from homogeneous metastable states, both the frequency factor and the heat of activation of the specific rate constant (2-2) can be calculated, although absolute intensities are not measured. Two theoretical monomolecular glow curves calculated from (5-2) are shown in Fig. 14.

In the case of luminescence involving activated,

rate-determining migration through the conduction band, bimolecular kinetics result. The notation is modified as follows: n_2 and n_{20} as the numbers of electrons in the conduction band at times t and t_0, and k_2' as the specific rate constant for the activated bimolecular process. The emission intensity is:

$$I_2 = -\alpha\frac{dn_2}{dt} = \frac{\alpha n^2{}_0 k_2'}{\left[1+\dfrac{n_{20}}{dT/dt}\displaystyle\int_{T_0}^{T} k_2' dT\right]^2}. \quad (5\text{-}5)$$

Assuming that a negligible number of electrons undergo radiationless recombination with the ionized center and that retrapping is again trivial, k_2' is obtained in terms of the "light sum":

$$k_2' = \frac{d}{dT}\left\{\alpha\left(\frac{dT}{dt}\right)^2 \frac{\displaystyle\int_{T_0}^{T} I_2 dT}{\displaystyle\int_{T}^{\infty} I_2 dT \int_{T_0}^{\infty} I_2 dT}\right\}. \quad (5\text{-}6)$$

It is clear from (5-6) that unless absolute intensities are measured only the heat of activation and not the frequency factor of the specific rate constant can be calculated from an experimental glow curve resulting from a bimolecular, rate-determining process. Two theoretical bimolecular glow curves calculated with (5-6) are shown in Fig. 15. These curves, like the monomolecular glow curves of Fig. 14, are not symmetrical. The bimolecular curves are skewed towards the low temperature, whereas the monomolecular curves are skewed toward the high temperature.

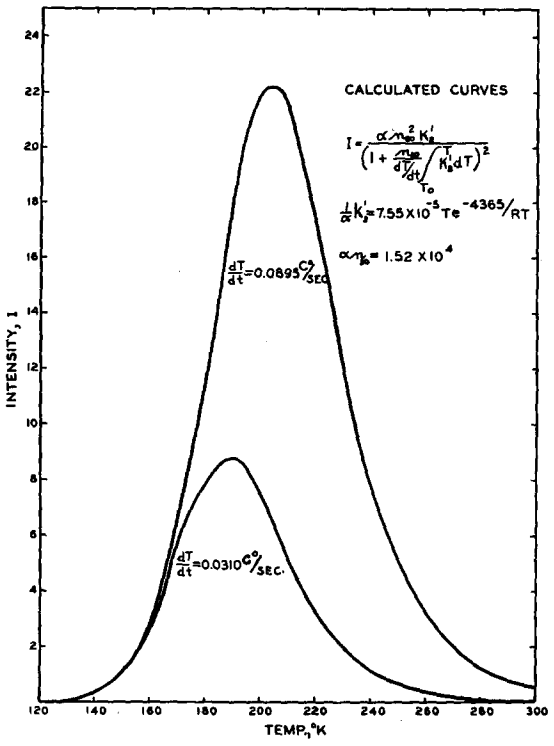

FIG. 15.

For the general treatment involving both monomolecular and bimolecular rate-determining processes, the following is the expression for the emission intensity assuming that the electrons in the conduction band and in the metastable state are in equilibrium according to the Boltzmann law:

$$I = \alpha k_1'\left\{\frac{k_1'/k_2' e^{2\epsilon/kT} n_{10}}{n_{10}\left[\exp\displaystyle\int_{t_0}^{t}\left(\frac{k_1'}{e^{-\epsilon/kT}+1}\right)dt - 1\right] + \dfrac{k_1'}{k_2'} e^{2\epsilon/kT} \exp\displaystyle\int_{t_0}^{t}\left(\frac{k_2'}{e^{-\epsilon/kT}-1}\right)dt}\right\}$$
$$+\alpha k_2'\left\{\frac{k_1'/k_2' e^{\epsilon/kT} n_{20}}{n_{20}\left[\exp\displaystyle\int_{t_0}^{t}\left(\frac{k_1' e^{\epsilon/kT}}{e^{\epsilon/kT}+1}\right)dt - 1\right] + \dfrac{k_1'}{k_2'} e^{\epsilon/kT} \exp\displaystyle\int_{t_0}^{t}\left(\frac{k_1' e^{\epsilon/kT}}{e^{\epsilon/kT}+1}\right)dt}\right\}^2, \quad (5\text{-}7)$$

where ϵ is the difference in energy between the conduction band and the metastable state. Because of the complicated nature of (5-7), (5-2), and (5-5) which treat the monomolecular and bimolecular mechanisms separately will be applied to experimental glow curves.

In applying the theoretical expressions for either monomolecular or bimolecular luminescence to experimental glow curves, the following procedure is used: The monomolecular case utilizing (5-1) to (5-4) will be applied first. As shown in the lowest section of Fig. 16, which is

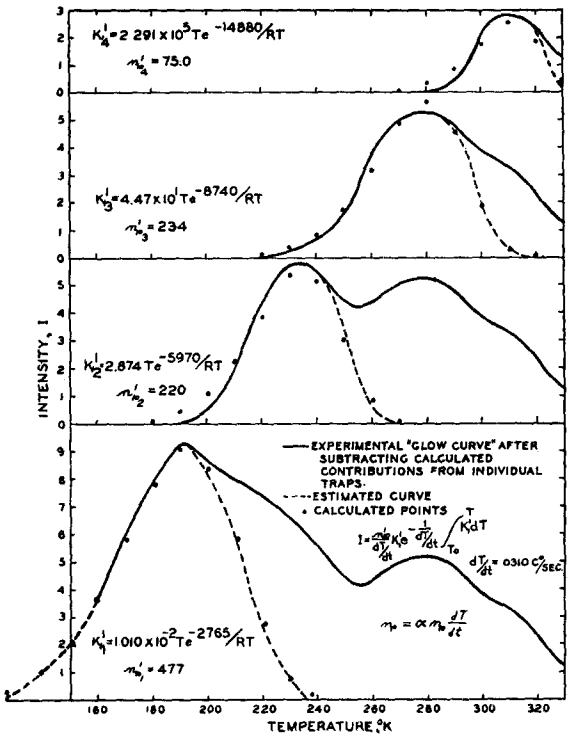

FIG. 16.

based on the glow data shown in Fig. 13, an estimate is made of the high temperature side of the emission intensity contributions from the low temperature peak. By measuring the area under the individual glow peak, a tentative total light sum from the particular metastable state is obtained. The area is also measured up to various temperatures to obtain the partial light sums that are a function of number of electrons that have been released before attaining the temperature in question. The light sums are inserted in (5-4), and a tentative specific rate constant is obtained graphically. The explicit form of the rate constant is substituted in (5-2) and the individual glow peak is calculated and compared with the experimental low temperature side and the estimated high temperature side. The light sums are redetermined to a second approximation, and the above procedure is repeated until the calculated glow peak fits the experimental and estimated curve. Insofar as the experimental, low temperature side of the glow peak is reproduced by the calculated curve, it is concluded that the high temperature side is also fitted. Figure 14 and the lowest section of Fig. 16 show the results of the third approximation.

A similar procedure was also repeated to the third approximation assuming a bimolecular, rate-determining process. The resulting theoretical glow peak is shown in Fig. 15. Because of the dependence of the shape of the build-up of peak emission on the order of the reaction, it is impossible to fit the initial part of the experimental glow curve assuming bimolecular kinetics. It is concluded that either the last remnant of a lower temperature glow peak is contributing or the rate-determining process is predominantly monomolecular.

Comparing (5-2) and (5-5), it is apparent that the emission is a different function of rate of heating for monomolecular and bimolecular processes. The temperature at which the maximum emission occurs depends on the rate of heating. The glow peak for the faster rate of heating can be calculated from the specific rate constant obtained by the analysis of the experimental glow curve at the slower rate. This can be done by assuming either a monomolecular or a bimolecular rate-determining mechanism. In the former case the maximum occurs at 213°K as shown in Fig. 14; in the latter case, the maximum occurs at 203°K as shown in Fig. 15. Because the experimental maximum for the faster rate of heating occurs at 208°K, it would appear that a mixture of monomolecular and bimolecular kinetics are involved. The simultaneous occurrence of photo-conductivity and luminescence favors at least a small bimolecular contribution. However, the shape of the initial portion of the experimental glow curve and the greater likelihood that an electron remains most of the time in a metastable state rather than in the conduction band favors an almost-exclusively monomolecular mechanism.

Having fairly conclusively established that the low temperature peak of the glow curve for ZnS:Cu is caused by a metastable state emptying by predominantly monomolecular kinetics, the remainder of the glow curve can now be analyzed. It is assumed that the remainder of the electron traps also empty by predominantly monomolecular kinetics, that all the traps empty independently, and that retrapping is negligible. Starting with the peak at the low temperature,

each metastable state is treated and subtracted from the experimental curve as shown in Fig. 16. The explicit expression for the specific rate constants and the relative numbers of electrons in the various metastable states are shown in Fig. 16. Summing up the emission contributions, the original glow curve is compared in Fig. 17 with the calculated expression:

$$I=\sum_i \alpha n_{i0} k_i' \exp\left(-\frac{1}{dT/dt}\int_{T_0}^{T} k_i' dT\right). \quad (5\text{-}8)$$

It is clear that, although the experimental and theoretical curves do not coincide precisely, sufficient recalculations would result in complete agreement.

The specific rate constants for the release of electrons from metastable states and the atomic rearrangements are characterized by low frequency factors and heats of activation between 2 and 15 kcal. The low values of the non-exponential part of the specific rate constant, between one and 10^8 per second, can be explained by two effects: Although, as shown in our model in Fig. 3, there is a rearrangement of the center during the release of an electron from a metastable state, it is primarily the electron that undergoes a change of state. Electrons are prone to "tunnel" through potential barriers or at least to pass through the barriers below their maxima. Such a process would have a smaller transmission probability than ordinary chemical reactions. An additional factor that reduces the frequency factor associated with the release of electrons from metastable levels is that the electron on surmounting or passing through the potential barrier undergoes some change in multiplicity. In other words, as shown in Fig. 3 the metastable and emitting states have somewhat different multiplicities, so that, in passing over or through the barrier an alteration of electron spin must occur. This is to some extent forbidden, so that a low transmission coefficient results.[22] Incidentally, it should be pointed out that the presence of two or more metastable states that are emptied by practically the same specific rate constants would, if not resolved, produce the same effect as a single metastable state with a smaller heat of activation and a smaller frequency coefficient. This substantiates the argument that the slowest linear rates of heating that give measurable emission intensities are desired in order to resolve individual metastable levels.

At constant temperature, the phosphorescence of luminescent materials having a number of discrete metastable states, such as the phosphors exhibiting glow curves of the type shown in Fig. 13, should proceed according to a summation of exponential functions:

$$I=\sum_i \alpha n_{i0} k_i' \exp(-k_i' t). \quad (5\text{-}9)$$

An expression of this type for approximately equally weighted metastable states, resulting in a fairly uniform distribution of specific rate constants, provides a markedly concave-upward afterglow that can be approximated by a hyperbolic function. In addition, since each specific rate constant in the summation has its own temperature dependence, the total phosphorescence curve will have a small irregular temperature dependence.

VI. CONCLUDING REMARKS

The purpose of this paper is to demonstrate that apparently unrelated diverse properties of luminescent solids can be quantitatively correlated in terms of a simple configuration coordinate diagram. In addition, deduction from the model shown in Fig. 3 indicates the direction that future experimental work should take.

For example, the lifetimes of the excited states provide some indication of the extent that the

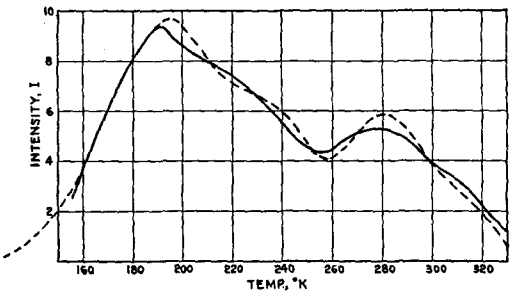

FIG. 17. — experimental "glow curve." -- calculated "glow curve."

$$I=\Sigma_i \alpha n_{i0} k_i' \exp\left(-\frac{1}{dT/dt}\int_{T_0}^{T} k_i' dT\right).$$

[22] C. Zener, Proc. Roy. Soc. **137**, 696 (1932); **140**, 660 (1933).

transitions are forbidden, but to determine the precise differences in multiplicities of the states involved, magnetic susceptibility measurements during different stages of excitation are necessary. ZnF_2:Mn is particularly well-adapted to such an experimental project because of its capacity to be excited to high concentrations of excited centers and to be evaporated and condensed in a vacuum to form thin transparent deposits without the loss of high luminescent efficiency.[23]

The absolute energies of the various excited states are needed to describe the model completely. Photo-conductivity measurements simultaneous with luminescent measurements will reveal the energies of the conducting excited states. Ultraviolet absorption data coupled with photo-conductivity data will reveal the non-conducting "exciton" states. Infra-red stimulation and quenching measurements on excited phosphors provide the optical depths of the metastable states. This information can be correlated with the thermal depths of the metastable states as obtained from the temperature dependence of phosphorescence and from glow data. For example, the heat of activation for release from the metastable state in the case of (Zn, Mg)F_2:Mn is about 4.5 kcal. indicating that this phosphor should be stimulated at $<6.3\mu$ if a radiationless process does not interfere.

A useful test of the applicability of the model would be an attempt to correlate for infra-red-sensitive phosphors diverse properties on the basis of a configuration coordinate diagram. With such phosphors some of the electron traps are very deep, and so, pronounced temperature dependence of efficiency is predicted.

This paper does not touch on the efficient mechanism for the transfer of energy from the lattice to the activator with corpuscular excitation. An analysis of this stage of the luminescent process depends on a knowledge of the mechanism of excitation and de-excitation of the activator. Based on the analysis of excitation and de-excitation phenomena presented in this paper, a semi-empirical treatment of the transfer of energy to the activator might be attempted by utilizing experimental results obtained with different types of excitation.

The authors are particularly indebted to Dr. R. E. Shrader of the RCA Laboratories for advice on the experimental work, for the use of apparatus, and in some instances for actual measurements. One of the authors (F.E.W.) would like to express his appreciation to Dr. V. K. Zworykin, Director of Electronic Research of the RCA Laboratories, for permitting him to work independently during this project.

[23] F. E. Williams, J. Opt. Soc. Am. **36**, 353 (1946).